

Ferroic properties in $\text{K}_{0.45}\text{Na}_{0.49}\text{Li}_{0.06}\text{NbO}_3$ ceramics

Laijun Liu^{*a}, Danping Shi^a, Longlong Fan^b, Jun Chen^b, Shaoying Zheng^a, Guizhong Li^a,
Aimei Yang^a, Liang Fang^a, Brahim Elouadi^c

^aKey laboratory of Nonferrous Materials and New Processing Technology, Ministry of Education, College of Materials Science and Engineering, Guilin University of Technology, Guilin 541004, China

^bDepartment of Physical Chemistry, University of Science and Technology Beijing, Beijing 100083, China

^cLaboratory of Chemical Analysis Elaboration and Materials, Engineering (LEACIM), Université de La Rochelle, Avenue Michel Crépeau, 17042 La Rochelle, Cedex 01, France

Abstract

Ferroelectric and magnetic properties of Fe-doped $\text{K}_{0.45}\text{Na}_{0.49}\text{Li}_{0.06}\text{NbO}_3$ (KNLN) and Cu-doped KNLN ceramics were investigated. Comparing with pure KNLN ceramic, Fe-doped KNLN shows ferromagnetic and ferroelectric properties simultaneously while Cu-doped KNLN diamagnetic and ferroelectric properties. Furthermore, a weak memory magnetoresistance effect was observed in Fe-doped KNLN at room temperature by the application of a magnetic field of 2 kOe. The magnetic properties in KNLN matrix are believed to be defect induced. The ferromagnetism of Fe-doped KNLN can be explained by the F-center exchange mechanism, while the diamagnetism of Cu-doped KNLN attributes to the special defect structure and Jahn-Teller effect of Cu^{2+} ion.

Keywords: Perovskite; Multiferroics; Jahn-Teller effect

* Corresponding author: Tel.: +867735893395; fax: +867735896290. Email: ljliu2@163.com (L. Liu)

INTRODUCTION

Much attention has been focused on perovskite oxides (ABO_3) due to their relatively simple structure and many excellent physical properties^[1], such as superconductive, giant dielectric, giant magnetoresistance and ferroelectric. For ferroelectric materials, spontaneous electric polarization can be switched to its symmetry equivalent states with applied electric field. The switchability of direction of polarization under electric field makes them useful in non-volatile memories while their sensitivity to stress and strain fields is responsible for piezoelectric devices. If the electrical polarization is coupled with magnetic field as well, the range of applications for ferroelectric materials could be greatly extended^[2]. Materials like this are called “multiferroics” that exhibit ferroelectricity and ferromagnetism under the same physical conditions, which is a fundamentally interesting property.

However, very few single-phase bulk materials have been found to be multiferroics at room temperature. Most perovskite ferroelectrics include transition metal ions with empty d shells, such as Nb^{5+} and Ti^{4+} at B site, which seem to be a prerequisite for ferroelectricity^[3]. In contrast, magnetism requires transition metal ions with partially filled d shells, such as Mn^{3+} and Fe^{3+} ^[4]. In perovskite oxides such as $BiFeO_3$ ^[4,5] ferroelectricity results from the stereochemically active 6s lone-pair of Bi^{3+} ions, and the magnetism arises from interacting spins of the d -electrons of Fe^{3+} ions. In manganites, such as $YMnO_3$, ferroelectricity is related to the geometry of its structure^[6].

In recent years, the interest of many researchers focuses on the substitution of magnetic ions at B site and creation of oxygen vacancies to induce magnetism in perovskite ferroelectrics such as $PbTiO_3$ ^[7], $BaTiO_3$ ^[8,9] and $K_{0.5}Na_{0.5}Nb_{0.95}Ta_{0.05}O_3$ ^[10].

However, the influence of defect characteristic on the coupling between magnetism (or diamagnetism) and ferroelectricity is not almost considered. This motivated us to explore the relationship between substitution ions with oxygen vacancies and the influence of point defects on the magnetism and ferroelectricity in perovskites. The selected material is $K_{0.45}Na_{0.49}Li_{0.06}NbO_3$ (KNLN), a lead-free piezoelectric material with excellent piezoelectric and ferroelectric properties^[11]. Here, we report the observation of room-temperature ferromagnetism and diamagnetism as well as ferroelectricity in iron doped KNLN and copper doped KNLN ceramics, respectively.

EXPERIMENTAL PROCEDURE

$K_{0.45}Na_{0.49}Li_{0.06}NbO_3$ (KNLN), $K_{0.45}Na_{0.49}Li_{0.06}NbO_3$ -1mol%Fe (KNLN-Fe) and $K_{0.45}Na_{0.49}Li_{0.06}NbO_3$ -1mol%Cu (KNLN-Cu) ceramics were prepared by the conventional solid reaction method. High-purity (99.99%) K_2CO_3 , Na_2CO_3 , Li_2CO_3 , Nb_2O_5 , Fe_2O_3 and CuO were used as raw materials. The weighted materials were milled with Y-doped ZrO_2 balls for 8h using ethanol as a medium and then calcined at $850^\circ C$ for 2h. The calcined powder was dried and milled again for 8h, and then pressed into pellets of 12mm in diameter. The pellets were sintered at a temperature range from 1020 to $1150^\circ C$ for 2h.

Bulk densities were determined by the Archimedes immersion technique and shown in Table 1. Phase identification of the ceramics was examined by X-ray diffraction (XRD; PANalytical X'pert PRO MPD) with $Cu K_{\alpha 1}$ radiation. Samples were polished and painted with silver paste on both sides, and then fired at $550^\circ C$ for 30 min. The room-temperature ferroelectric properties at 1 Hz were measured using the ferroelectric testers (aixACCT:

TF-2000). Small bulks ($1 \times 1 \times 1 \text{ mm}^3$) were cut from the as-prepared samples for magnetic property measurements and magnetization-field curves were achieved using physical property measurement system (PPMS; Quantum Design). The capacitor and conductivity with or without applied magnetic field were measured using Precision LCR Meter at room temperature.

RESULTS AND DISCUSSION

XRD patterns of the KNLN, KNLN-Fe and KNLN-Cu ceramics are shown in Fig. 1. Both doped samples possess a single monoclinic perovskite structure and no impurity can be found, indicating that most of iron and copper ions diffuse into the host lattice. Since all samples were sintered in air and not annealed in oxygen atmosphere, vapor, or vacuum, Fe ions should maintain their raw valence of $3+$ ^[12] while Cu ions should be $2+$ ^[13], which was proved by many researchers using electron paramagnetic resonance (EPR). The ionic radii of Fe^{3+} (0.55 Å for LS and 0.645 Å for HS) Cu^{2+} (0.73 Å) ions are very similar to the Nb^{5+} ion (0.64 Å) and much smaller than that of the Na^+ ion (1.39 Å) and K^+ ion (1.64 Å), therefore, it is reasonable to imply that transition metals ions substitute into the Nb sites of KNLN lattice. The structure of the ceramics was refined by using the XRD Rietveld method supported by the software TOPAS^[14]. The cell parameter and cell volume were obtained (Table 1) according to *Pm* (group 6) space group. KNLN-Cu has the maximum cell volume. It could associate with defect structure (oxygen vacancy and Jahn-Teller effect), we will discuss later.

The microstructure of thermally etched ceramics was investigated by scanning electron microscope (SEM, JEOL JSM-6380LV). Our studies concentrated on the effect

of dopants on the final microstructure. SEM images of KNLN-based ceramics with different dopants are presented in inset of Fig. 1. An average grain size of 10–15 μm was obtained for these samples (Table 1). Homogeneity varies slightly between the different compositions while KNLN-Fe shows a cuboid morphology. However, the difference between the homogeneity and grain size of the different compositions is not significant enough to conclude there is any influence of composition. The fine-grained microstructure is quite uniform with few grain-boundary porosities.

Polarization hysteresis loops of the KNLN, KNLN-Fe and KNLN-Cu ceramics were measured at room temperature and 1 Hz, as shown in Fig. 2. Their curves show saturation polarization when applied electric field is 4 kV/mm. The electric coercive field (E_c) and remanent polarization (P_r) of the KNLN ceramics are 0.95 kV/mm and 20.6 $\mu\text{C}/\text{cm}^2$, respectively. After the addition of 1 mol% iron element, the loop becomes slanted with $E_c = 1.20$ kV/mm, $P_r = 10.7$ $\mu\text{C}/\text{cm}^2$. Unlike KNLN and KNLN-Fe, the KNLN-Cu ceramic exhibits a double P - E loop at 1 Hz, which associates with the symmetry-conforming principle of point defects^[15]. We will discuss it latter. The increase in E_c and decrease in P_r indicate that Fe^{3+} and Cu^{2+} act as an acceptor in KNLN ceramics, which is consistent with ref. 12 and 13. Because the valence of iron and copper is lower than that of niobium at B site, oxygen vacancies shared with nearby unit cells will be formed in order to maintain the charge neutrality. These oxygen vacancies pin the domain wall motion thus make ferroelectric properties weaken.

Magnetic properties of the KNLN-Fe and KNLN-Cu ceramics were measured at different temperatures. The KNLN-Fe ceramic shows ferromagnetism with hysteresis loops shown in Fig. 3(a1), confirming the existence of ferromagnetic long-range order.

The temperature dependence of saturation magnetization for the KNLN-Fe ceramic at zero-field cooled (ZFC) and 0.5T field cooled (FC) conditions in the temperature range from 15 to 390K is shown in Fig. 3(a2). A sharp decrease of magnetization with increasing temperature can be found below ~50K then a linear decrease presents up to 390K, where both ZFC and FC branches overlap over the whole temperature range. The ferromagnetism of KNLN-Fe could be explained by the F-center exchange mechanism (FCE).^[16,17] An electron trapped inside the oxygen vacancy constitutes an F-center, and the exchange interaction between two Fe³⁺ ions nearby via the F-center brings about the ferromagnetism.

In contrast to KNLN-Fe, KNLN-Cu ceramic shows diamagnetism with similar hysteresis loops at different temperatures, shown in Fig. 3(b1). The KNLN ceramic is diamagnetism can be seen in the inset part of Fig. 3(b1). It is clear that diamagnetic property will be enhanced with the introduction of Cu ion. Therefore, a different exchange interaction between point defects from KNLN-Fe could contribute to the diamagnetic property. The temperature dependence of magnetization for KNLN-Cu ceramic at ZFC/FC in a temperature range from 15 to 390K is shown in Fig. 3(b2). The absolute value of magnetization increases rapidly with the increase of temperature below 100K then decreases slightly up to 390K, meanwhile, ZFC and FC curves do not overlap in the temperature range from 100 to 390K.

The difference of magnetic performance between KNLN-Fe and KNLN-Cu should result from defect structure and ion characteristic. For the KNLN-Cu, the enhanced diamagnetism may be related to the Jahn-Teller distortion of Cu²⁺O₆ octahedron due to the induced Cu²⁺ Jahn-Teller ion doping at Nb⁵⁺ (not a Jahn-Teller ion) site. The

distortion could be one of reason to result in maximum cell volume. In addition, the defect structure should be taken into account for understanding the diamagnetism. Eichel et al ^[13] analyzed the defect structure of KNLN-Cu ceramics by electron paramagnetic resonance (EPR) spectroscopy. The results indicate that Cu preferentially substitutes on the Nb sites where it can trap one or two oxygen vacancies. Two types of defect associates are formed $(Cu_{Nb}''' - V_O^{''})'$ and $(V_O^{''} - Cu_{Nb}''' - V_O^{''})^{\bullet}$, which is different from that of KNLN-Fe ^[16]. Owing to the opposite charges of these two types of defects, overall charge neutrality is theoretically possible by mutual compensation of the defect associates, without formation of additional non-associated oxygen vacancies. For the latter type, the Cu^{2+} ion should relax back into the plane spanned by the four equatorial oxygens ^[18] (which agrees with Jahn-Teller distortion). As a consequence, the distance to the two oxygen vacancies are approximately equal, and the electric dipole moment for that defect associate almost vanishes. The special defect structure is also the origin of double-hysteresis loop of KNLN-Cu.

In the condition of defect $(Cu_{Nb}''' - V_O^{''})'$, Cu^{2+} lies in an asymmetric environment in an octahedron, which would lead to an additional $Cu^{2+}O_6$ octahedron distortion besides the distortion from the Jahn-Teller effect. The variation of $Cu^{2+}O_6$ octahedron distortion results in the rotation of the orbit. The force generated by the orbit rotation makes the spin tilt due to the spin-orbit coupling. As a result, the vector sum of individual spins may orient along or opposite to the direction of the applied magnetic field. Macroscopically, the average magnetization exhibits positive or negative values ^[19].

The Cu^{2+} ions with nine d -electrons in the valence shell (t_{2g} and e_g) in an octahedral environment with six equivalent atoms in the first coordination sphere constitute a classic

example of Jahn-Teller systems. For such Cu^{2+} complexes, dynamic Jahn-Teller behavior is commonly observed at room temperature^[20]. On lowering the temperature, the dynamic behavior is likely to vanish below a temperature called the Jahn-Teller transition temperature and a static distortion occurs. These distortions depend strongly on the matrix of the ligand as well as on the geometrical environment^[21]. This can explain $M(T)$ curves of KNLN-Cu at ZFC/FC overlap at low temperature and separate at high temperature.

Considering the coexistence of ferroelectric, diamagnetic and ferromagnetic orders in the KNLN-Fe and KNLN-Cu ceramics, one can expect the coupling between ferroelectricity and ferromagnetism. Fig. 4 shows capacitance (C) and admittance (G) as a function of frequency at zero field and $H=2$ kOe field for KNLN-Fe (4a) and KNLN-Cu (4b) ceramics. A slight increase of capacitance occurs in KNLN-Fe sample (Fig. 4a1) at low frequency while no change in KNLN-Cu sample (Fig. 4b1) in the whole frequency. Furthermore, KNLN-Fe shows magnetoresistance effect (Fig. 4a2) in a very broad frequency range. The effect can be remained when the magnetic field removes, indicating that it is memorial. The effect of magnetic field on capacitance and resistance indicates the strong coupling between the ferroelectric and ferromagnetic orders in KNLN-Fe. But for KNLN-Cu, the coupling is not clear (Fig. 4b2) due to the special defect structure and Jahn-Teller effect of Cu ion. Therefore, defect type and ion characteristic are the keys to control the coupling between the ferroelectric and ferromagnetic in perovskite ferroelectrics.

In summary, we experimentally proved the unusual magnetic properties in the Cu-doped KNLN ceramics whereas pure KNLN exhibits very weak diamagnetism. The

magnetic hysteresis loops are clearly observed in the temperature range of 15 K to 390 K and present great difference between Fe-doped KNLN and Cu-doped KNLN. Further studies on ferroelectric, ferromagnetism and diamagnetism properties in other perovskite oxides are highly expected. The present experimental results are expected to open up new possibilities in the investigations of the physical mechanism and the multiferroic application for the perovskite oxides as well as spin electronics.

Acknowledgements

This work was supported by Natural Science Foundation of China (No. 11264010, 51002036, 50962004, 21061004 and 51102058), the Project of Department of Science and Technology of Guangxi (No. 12118017-13) and the Natural Science Foundation of Guangxi (Grant No. BA053007). We thank Dr. Jun Lu and Prof. Yicheng Cai (Institute of Physics, Chinese Academy of Sciences) for high temperature magnetization measurements.

References

- [1] M. A. Peña and J. L. G. Fierro, *Chem. Rev.* **101**, 1981 (2001).
- [2] J. F. Scott, *Nat. Mater.* **6**, 256 (2007).
- [3] R. E. Cohen, *Nature* **358**, 136 (1992).
- [4] J. Wang, J. B. Neaton, H. Zheng, V. Nagarajan, S. B. Ogale, B. Liu, D. Viehland, V. Vaithyanathan, D. G. Schlom, U. V. Waghmare, N. A. Spaldin, K. M. Rabe, M. Wuttig, and R. Ramesh, *Science* **299**, 1719 (2003).
- [5] J. B. Neaton, C. Ederer, U. V. Waghmare, N. A. Spaldin, K. M. Rabe, *Phys. Rev. B* **71**, 014113 (2005).
- [6] B. B. Van Aken, T. T.M. Palstra, A. Filippetti & N. A. Spaldin, *Nat. Mater.* **3**, 164

(2004).

- [7] V. R. Palkar and S. K. Malik, *Solid State Commun.* **134**, 783 (2005).
- [8] B. Xu, K. B. Yin, J. Lin, Y. D. Xia, X. G. Wan, J. Yin, X. J. Bai, J. Du, and Z. G. Liu, *Phys. Rev. B* **79**, 134109 (2009).
- [9] R. V. K. Mangalam, N. Ray, U. V. Waghmare, A. Sundaresan, C. N. R. Rao, *Solid State Commun.* **149**, 1(2009).
- [10] H. Li, W. Yang, Y. Li, Q. Meng, and Z. Zhou, *Appl. Phys. Express* **5**, 101501 (2012).
- [11] Y. Saito, H. Takao, T. Tani, T. Nonoyama, K. Takatori, T. Homma, T. Nagaya, and M. Nakamura, *Nature* **42**, 84 (2004).
- [12] A. P. Pechenyi, M. D. Glinchuk, C. B. Azzoni, F. Scardina, and A. Paleari, *Phys. Rev. B* **51**, 12165 (1995).
- [13] R. -A. Eichel, E. Erünal, M. D. Drahus, D. M. Smyth, J. van Tol, J. Acker, H. Kungl and M. J. Hoffmann, *Phys. Chem. Chem. Phys.* **11**, 8698 (2009).
- [14] L.B. McCusker, R.B. Von Dreele, D.E. Cox, D. Louer, P. Scardi, *J. Appl. Cryst.* **32**, 36 (1999).
- [15] D. Lin, K. W. Kwok, and H. L. W. Chan, *Appl. Phys. Lett.* **90**, 232903 (2007).
- [16] J. M. D. Coey, A. P. Douvalis, C. B. Fitzgerald, and M. Venkatesan, *Appl. Phys. Lett.* **84**, 1332 (2004).
- [17] Z. D. Dohčević-Mitrović, N. Paunović, M. Radović, Z. V. Popović, B. Matović, B. Cekić, and V. Ivanovski, *Appl. Phys. Lett.* **96**, 203104 (2010).
- [18] R.-A. Eichel, P. Erhart, P. Träskelin, K. Albe, H. Kungl and M. J. Hoffmann, *Phys. Rev. Lett.* **100**, 095504 (2008).

- [19] R. Ang, Y. P. Sun, Y. Q. Ma, B. C. Zhao, X. B. Zhu, and W. H. Song, *J. Appl. Phys.* **100**, 063902 (2006).
- [20] T. K. Kundu, P. T. Manoharan, *Chem. Phys. Lett.* **241**, 627 (1995).
- [21] K. V. Narasimhulu, C. S. Sunandana, J. L. Rao, *J. Phys. Chem. Solids* **61**, 1209 (2000).

Figure Captions

Table 1 Density, grain size and cell parameter of KNLN-base ceramics

- Fig. 1 XRD patterns of (a) KNLN, (b) KNLN-Fe and (c) KNLN-Cu ceramics and results of crystallographic refinement using the space group Pm . Inset, SEM micrographs of polished and thermal etched surfaces of sintered KNLN, KNLN-Fe, KNLN-Cu, respectively. The quality of fit of the refinements is shown at the right bottom of the picture.
- Fig. 2 Polarization hysteresis loops of the KNLN, KNLN-Fe and KNLN-Cu ceramics at room temperature and 1 Hz.
- Fig. 3 (a) Field dependence of magnetization for the KNLN-Fe (a1) and KNLN-Cu (b1) ceramics at different temperatures. KNLN-Fe shows ferromagnetism while KNLN-Cu diamagnetism. Inset, field dependence of magnetization of the KNLN, shows weak diamagnetism. (b) Temperature dependence of magnetization for the KNLN-Fe (a2) and KNLN-Cu (b2) ceramics at zero-field cooled (ZFC) and H=0.5T field cooled (FC).
- Fig. 4 Capacitance (C) and admittance (G) as a function of frequency at zero field and H=2 kOe field for KNLN-Fe (4a) and KNLN-Cu (4b) ceramics. A memorial magnetoresistance effect can be found in KNLN-Fe sample.

Table 1 Density, grain size and cell parameter of KNLN-base ceramics

Sample	Relative density	Average grain size	Cell parameter (Å)				Cell volume
			<i>a</i>	<i>b</i>	<i>c</i>	β	
KNLN	97.1%	12.3 μm	3.95448	3.93841	4.03701	90.06732	62.8740 Å ³
KNLN-Fe	95.7%	10.2 μm	3.99699	3.94035	4.00152	90.33288	63.0209 Å ³
KNLN-Cu	98.1%	14.8 μm	3.98713	3.94120	4.00632	90.30343	62.9546 Å ³

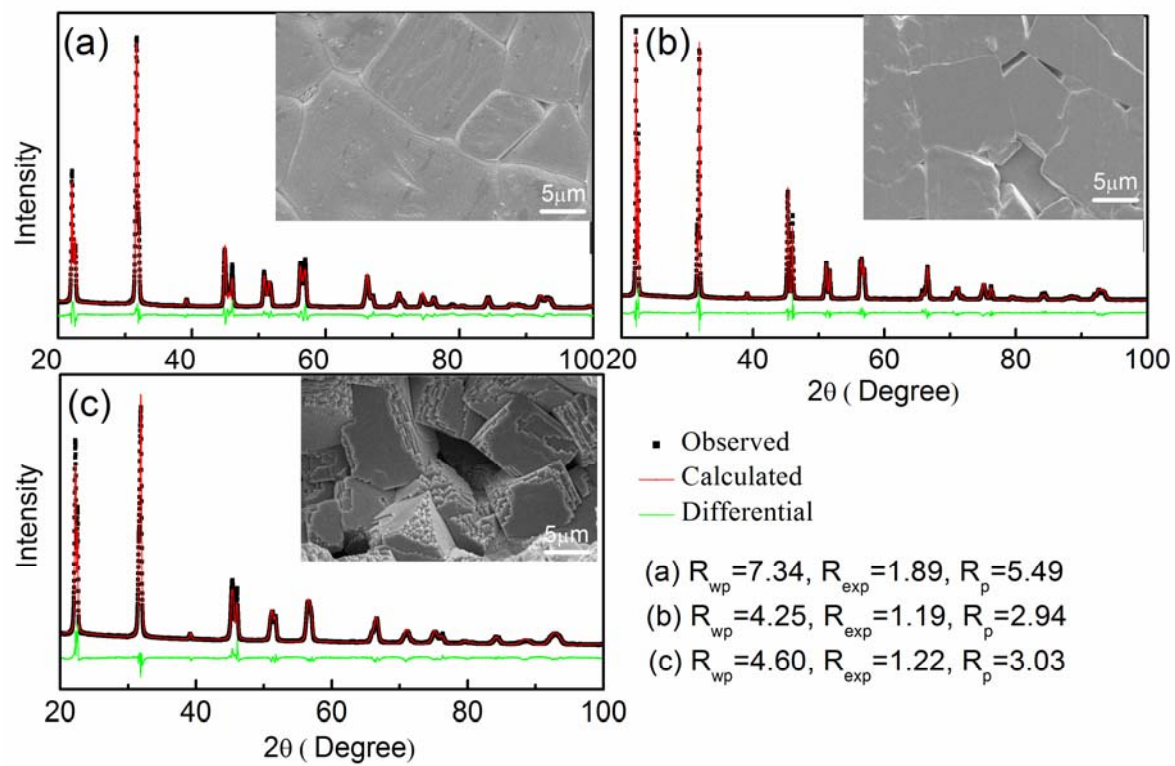


Figure 1

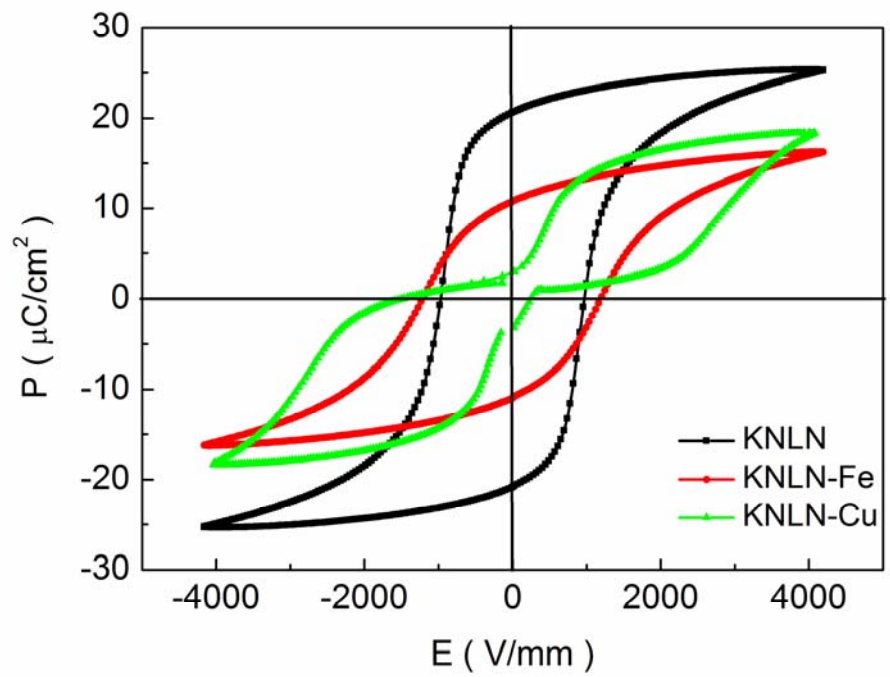


Figure 2

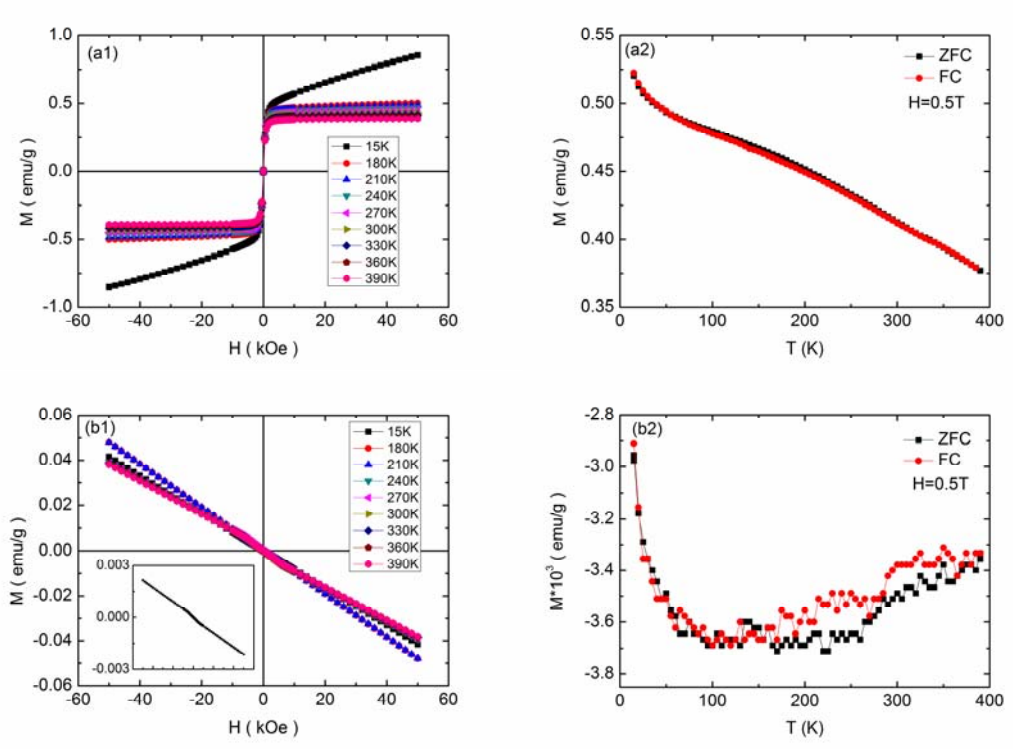


Figure 3

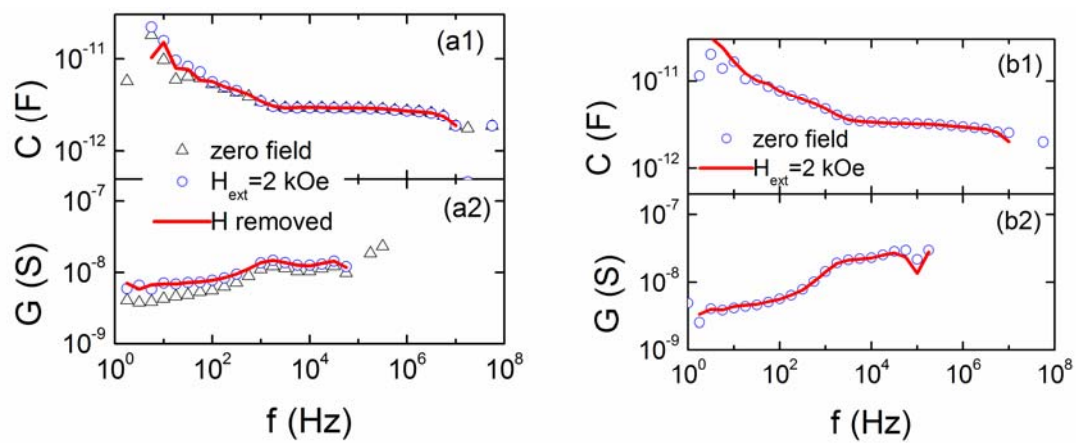


Figure 4